INTERNATIONAL JOURNAL OF
ENERGY AND ENVIRONMENT

Volume 9, Issue 5, 2018 pp.429-448
Journal homepage: www.IJEE.IEEFoundation.org

Natural convection in an air filled cavity with various heat source locations

Ahmed kadhim Hussein, Falah Hassan Naiem

College of Engineering, Mechanical Engineering Department, Babylon University, Iraq.

Received 19 Feb. 2018; Received in revised form 21 June 2018; Accepted 3 July 2018; Available online 1 Sep. 2018

Abstract
The numerical investigation of the natural convection in a vertical rectangular cavity filled with air is carried by using the finite difference method. The horizontal walls of the cavity are assumed adiabatic. While, the vertical walls are assumed partially heated. Two thermal sources were taken in this study. The hot source was installed in the left sidewall while, the cold was installed on the right sidewall. The sources localized at bottom – bottom position. The flow and thermal fields properties are computed for Rayleigh number ($103 \leq Ra \leq 106$), source lengths ($0.25 \leq Ls \leq 0.75$), and aspect ratio ($1 \leq AR \leq 2$) respectively. The results show that, when the Rayleigh number and aspect ratio increase, the fluid flow intensity in the cavity increases also. While, with changing the sources lengths by decrease in the hot source length and the increase in the cold source lengths can be used to improve the flow field. It's found that the Nusselt number was high with installing the hot source at the top region of the left sidewall while the cold source at bottom region of the right sidewall.

Keywords: Natural convection; Aspect ratio; Dimensionless heat source length.

1. Introduction

Convection is the transfer of thermal energy due to the motion of fluids. Natural convection is defined as the fluid flow and heat transport arising due to density and temperature differences in the fluid. This is different from forced convection where the transport is because of an external energy source like a fan or a pump [1]. In cavities the natural have wide applications in many thermal applications such as solar collectors, cooling devices in electronic appliances, energy storage devices and insulation of buildings[**2**].The first group of researchers was studied this problem in an cavity with differentially sidewalls. Examples of these studies were achieved by Cianfrini et al. [3], Basak et al. [4], Hussein and Hussain [5], Turan et al. [6] and Bhattacharya [7]. While, the second group of researches like Hasnaoui et al. [8], Calcagni et al. [9], Nasr et al. [10], Cheikh et al. [11] and Tablet et al. [12]. Were studied this problem in a cavity with one partially active sidewalls. Other researchers deal with two partially active sidewalls, this due to complexity of the numerical solution. Turkoglu and Yucel [13], performed a numerical study to investigate effects of both the heater and cooler locations on the convection inside a square air filled cavity. The left and right sizes of the heaters took about a quarter of the length of the vertical wall of the enclosure. It was found that the (Nu_{av}) was increased when the heater was moved towards the lower wall. Kandaswamy et al. [14], numerically studied the laminar natural convection in a

rectangular enclosure filled with various fluids. The left and right sidewalls of it were considered as partially thermal active walls. However, the top and bottom walls were considered adiabatic. The effects of (AR), (Gr), (P_r) and heat source locations were studied. They concluded that the maximum heat transfer occurred at the middle-location of the heat source. Alam et al. [15], numerically studied the natural convection in a rectangular enclosure due to partial heating and cooling sidewalls. The rest of the enclosure walls were considered insulated. The results were presented in terms of streamlines, isotherms and (Nu_{av}) for various values of (AR) and (Ra). They found that as (AR) and (Ra) increased, the (Nu) was increased too. Djoubeir et al. [16], numerically analyzed the natural convection in an air filled square cavity. Both the left, right and lower walls of it were subjected to a partial heat source. While, the other regions of these walls were considered cold. The upper wall of the cavity was kept adiabatic. They concluded that the effect of the heat source location was significant for $10^3 \leq Ra \leq 10^4$. Mahapatra et al. [17], numerically investigated the effect of active wall location on natural convection in a partially heated enclosure filled with air. Except for the partial regions of hot and cold walls, the remaining regions of the enclosure were kept insulated. Six different arrangements of the partial heating and cooling locations were considered .It was found that the bottom-bottom arrangement was suitable for good thermal mixing. However, the bottom-top one was useful for better temperature distribution.

2. Mathematical formulation

2.1 Geometry description

The geometry considered in the current paper is a vertical cavity with a two partially active sidewalls. The horizontal walls of the cavity are assumed adiabatic. While, the vertical sidewalls assumed partially heated. The case one, the lower regions of the left and right sidewalls of the cavity are subjected to a partial heating and cooling respectively. While, the case two have opposite locations of these thermal heat sources in vertical sidewalls from case one. The cavity are of height (H), width (W) (i.e., AR = H/W) as shown in Figure 1. The governing parameters for the considered cases are [$10^3 \leq Ra \leq 10^6$, $1 \leq AR \leq 2$ and $0.25 \leq L_S \leq 0.75$] respectively.

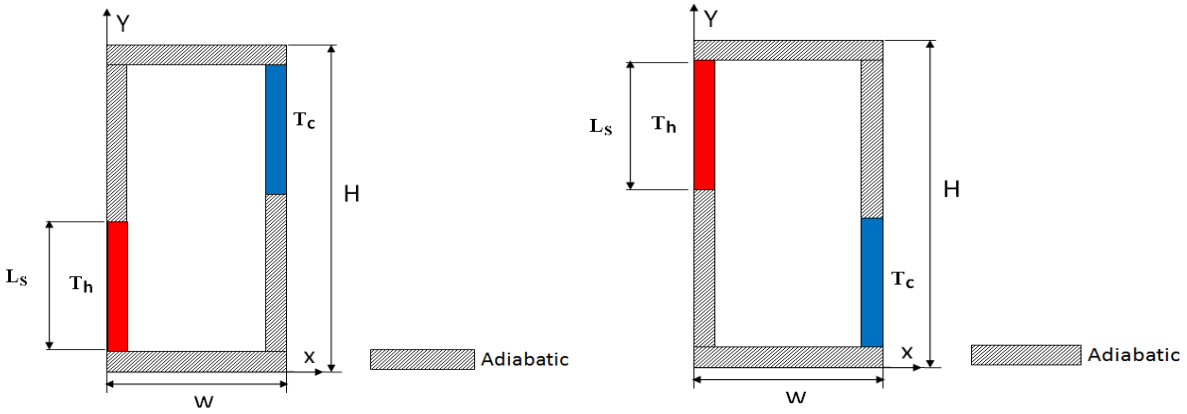

Figure 1. Physical domain and coordinate system for (B-T) and (T-B) cases.

2.2 Governing equations

In order to start the description of the governing equations, the following assumptions are included:

1. The flow is considered steady, two-dimensional, incompressible and laminar.
2. Radiation mode of the heat transfer is considered negligible.
3. Internal heat generation is neglected.
4. The fluid thermo-physical properties are assumed constant, except the density in the body force term in the momentum equation which is treated according to the Boussinesq approximation.

The dimensionless form of the governing equations which are used in the present work can be given as follows:

$$\frac{\partial U}{\partial X} + \frac{\partial V}{\partial Y} = 0 \qquad (1)$$

$$U\frac{\partial U}{\partial X}+V\frac{\partial U}{\partial Y}=-\frac{\partial P}{\partial X}+P_r\left(\frac{\partial^2 U}{\partial X^2}+\frac{\partial^2 U}{\partial Y^2}\right) \quad (2)$$

$$U\frac{\partial V}{\partial X}+V\frac{\partial V}{\partial Y}=-\frac{\partial P}{\partial Y}+P_r\left(\frac{\partial^2 V}{\partial X^2}+\frac{\partial^2 V}{\partial Y^2}\right)+(RaP_r\theta) \quad (3)$$

$$U\frac{\partial \theta}{\partial X}+V\frac{\partial \theta}{\partial Y}=\frac{\partial^2 \theta}{\partial X^2}+\frac{\partial^2 \theta}{\partial Y^2} \quad (4)$$

2.3 Boundary conditions

The boundary conditions in dimensionless form can be represented as illustrated in Figure 1.

2.4 Local Nusselt number

The local Nusselt number is calculated from the following equation:

$$Nu=-\left.\frac{\partial \theta}{\partial X}\right|_{(x0} \quad (5)$$

3. Numerical approach, validation and the grid independent examination

The software Fortran 90 was used this present work after it was validated by comparing with results of other researchers as shown in Figure 2. Then the result model was used to simulate the boundary condition suggested by the study as shown in figures below and to analyze the grid sensitivity. Tables 1 and 2 shows a refinement test of grids for two cases which is made for five uniform different grids (21*21),(31*31),(41*41), (51*51) and (61*61) with [Ra = 10^6 and AR = 1].

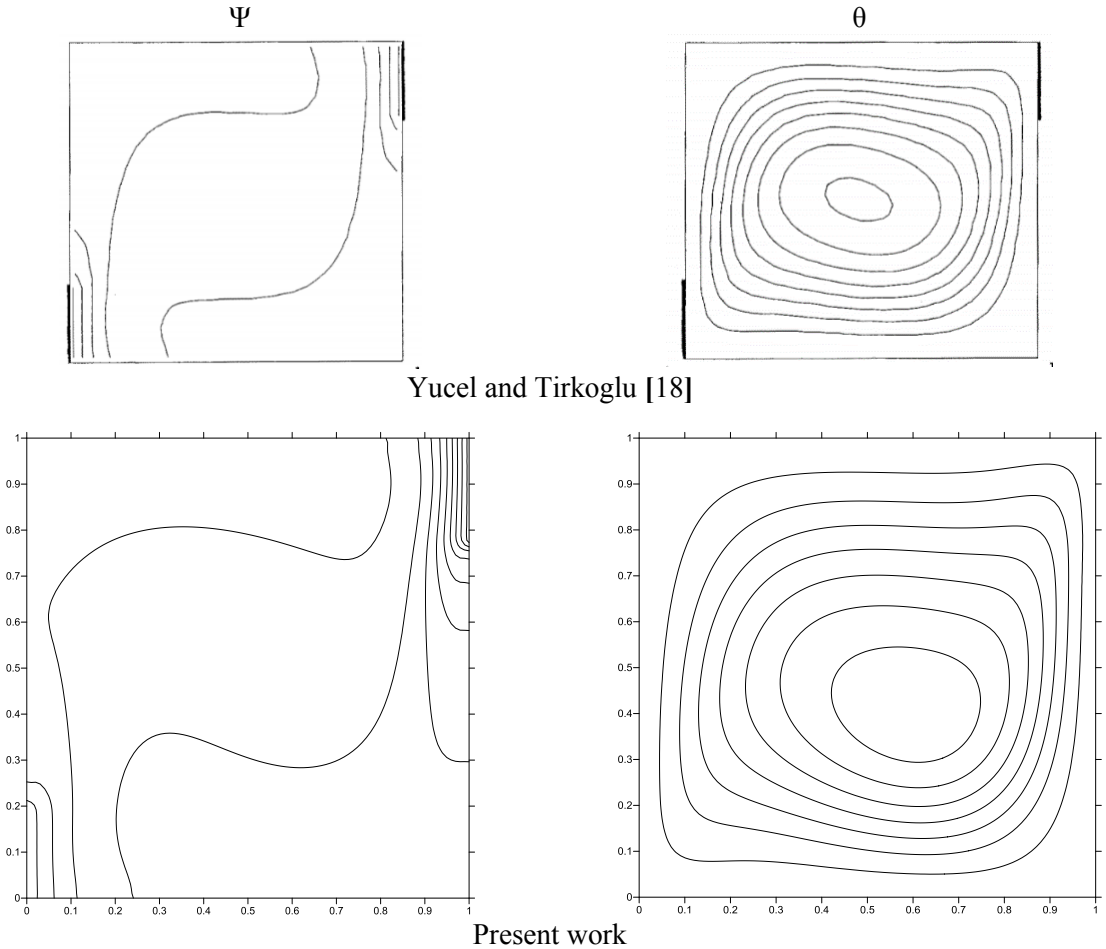

Figure 2. Comparison of streamlines (Ψ) and isotherms (θ) contours between Yucel and Tirkoglu [18] and the present work at [Φ = 90°, Ra =10^4 and AR=1].

Table 1. Results of grid independence test for bottom-top case 1.

Number of grid in X-Y plane	Nu	Error%
21*21	3.22	
31*31	3.18	1.25
41*41	3.17	0.31
51*51	3.15	0.63
61*61	3.12	0.96

Table 2. Results of grid independence test for bottom-top case 2.

Number of grid in X-Y plane	Nu	Error%
21*21	1.31	
31*31	1.28	2.34
41*41	1.27	1.12
51*51	1.25	1.60
61*61	1.23	1.62

4. Results and discussion

The problem of the natural convection in a vertical cavity with two partially heated sidewalls is analyzed numerically in this research.

4.1 Case one (bottom -top)

A- Effect of Rayleigh number

The studying of the effects of Rayleigh number on the flow and thermal fields is illustrated in Figure 3.The explaining of (Ra) on streamline contours for case (B-T) are taken for [AR= 1, L_h= 0.5 and L_c=0.25]. When the flow begins with (Ra = 10^3), the stream value is small [$|\Psi|_{max}$ = 0.46] and then it begins to increase with increasing of (Ra) to reaches its maximum value [$|\Psi|_{max}$ = 22] at (Ra = 10^6). This increasing due to the strong effects of convection with increasing of (Ra).In general, the flow is starting its motion with major vortices which is moved by vertical movement from the hot region at lower part of left sidewall towards the cold region at upper right sidewall passing beside the adiabatic horizontal walls. Anyway, after increasing (Ra) to (Ra = 10^6) the flow is construct from a minor vortices which are observed up to hot source and below the cold one. Also, in Figure 3 a clear change in the vortices shapes can be seen. It shifted and accumulated above the hot source and below the cold one respectively with deviation in their shapes near the both sources at lower and upper corners. This due to the high value of (Ra).

With respect to the isotherm, it can be seen from Figure 3a, that when (Ra) is low [i.e., Ra = 10^3], they are uniform in their shapes and parallel to each other. This due to the high effect of conduction heat transfer in cavity. After increasing the (Ra) to [Ra = 10^4 to 10^6] as shown in Figure 3b, their behavior becomes different. It begins to change near the hot source and extended to the top towards the cold source. Also, their shapes changed to curved horizontally especially at the middle of the cavity. This due to the increase in convection effects with increasing of (Ra).

B- The effect of aspect ratio of the cavity

Figures 4 and 5 illustrate the streamline (Ψ) and (θ) isotherm contours for various aspect ratio and Rayleigh number with [L_h = 0.5 and L_c = 0.25]. It can be noticed that with increasing the aspect ratio, the stream function increased from [$|\Psi|_{max}$ = 0.84] to [$|\Psi|_{max}$ = 1.1] at (Ra = 10^3) as shown in Figure 4 and from [$|\Psi|_{max}$ = 29] to [$|\Psi|_{max}$ = 36] at (Ra = 10^6) as shown in Figure 5. From these figures, it can see that the flow represented from a major vortices at (Ra = 10^3) while, it construct from major and minor vortices at [Ra =10^6].But in both values of (Ra) their shapes is not effected with increasing of aspect ratio. Therefore, it can be concluded that the increase in (AR) does not have a clear effect for (B-T) case.

With respect to isotherm contours, it can be seen that with increasing in (AR), the conduction heat transfer is controlled at (Ra = 10^3) as shown in Figure 4, while the convection is significant at (Ra = 10^6) as shown in Figure 5. So, it can be observed that the isotherm lines does not effected with increasing of aspect ratio. Therefore, this results lead to conclude that the effect of (Ra) on stream lines and isotherms is greater than the effect of (AR).This is noticed for this [B-T] case.

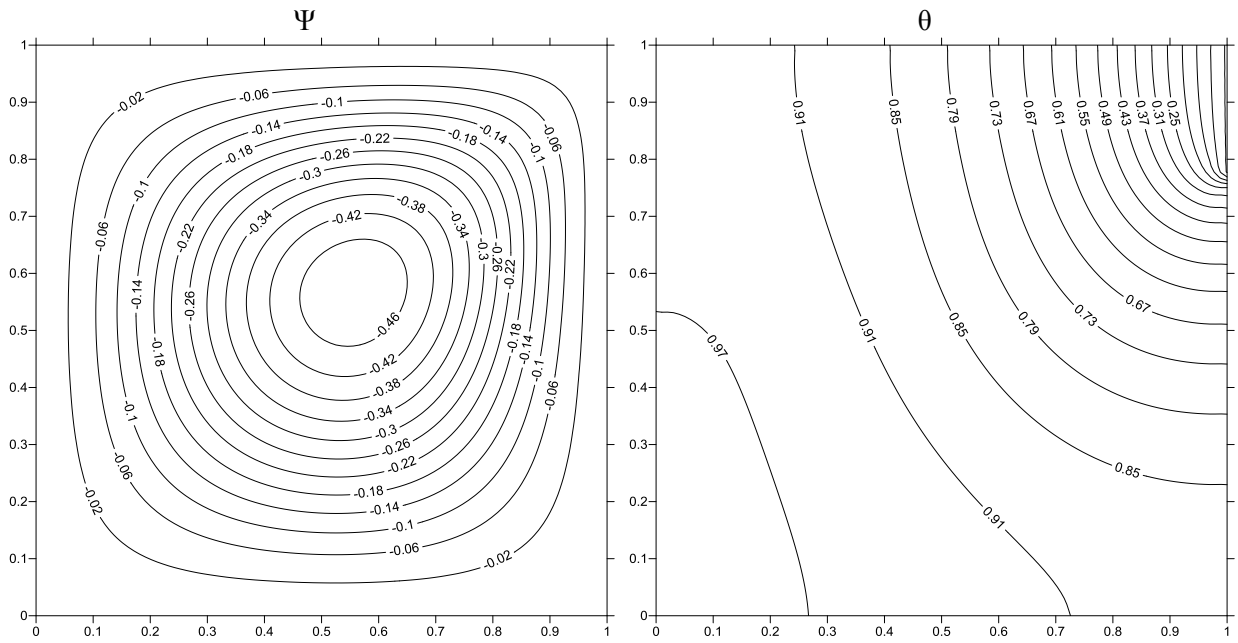

(a) Ra = 10^3

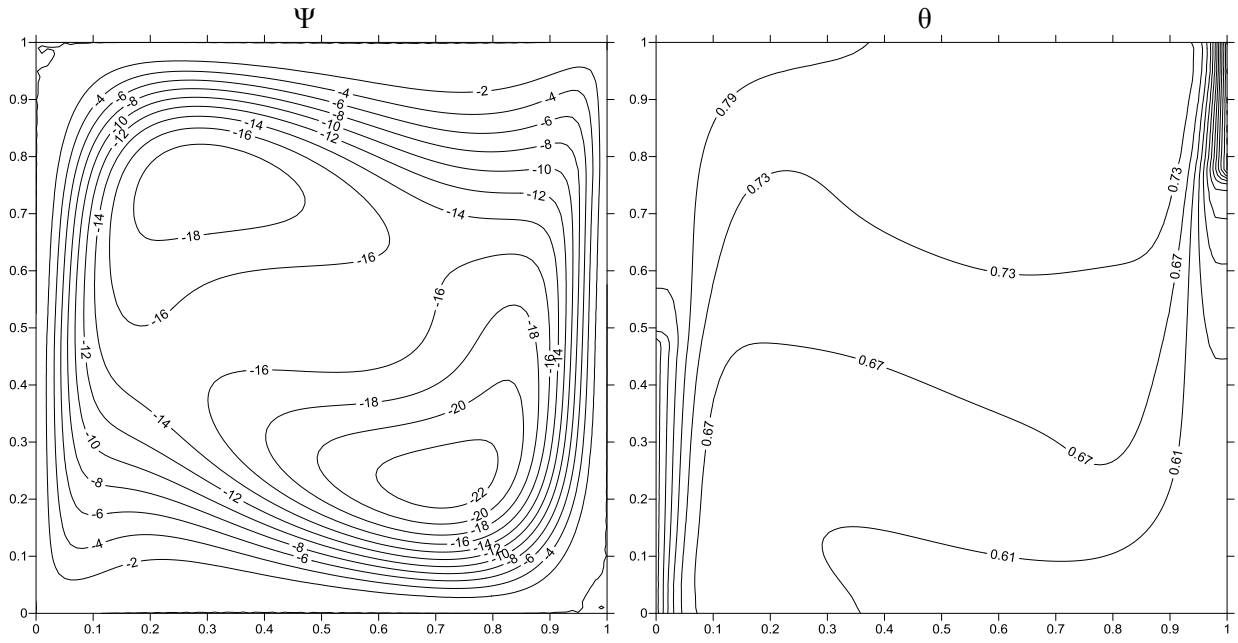

(b) Ra = 10^6

Figure 3. Streamline (Ψ) and isotherm (θ) contours of bottom-top case for various Rayleigh number and [AR=1, L_h = 0.5 and L_c = 0.25].

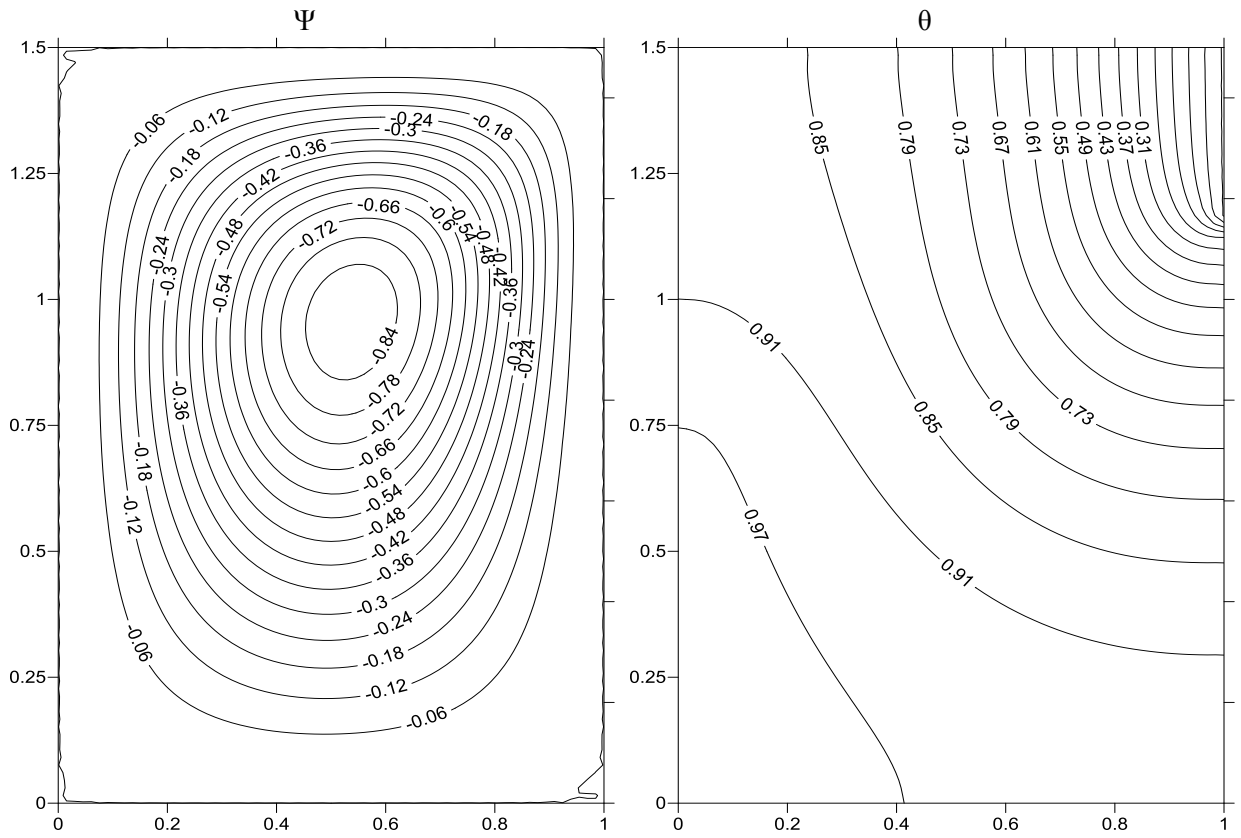

(a) AR = 1.5

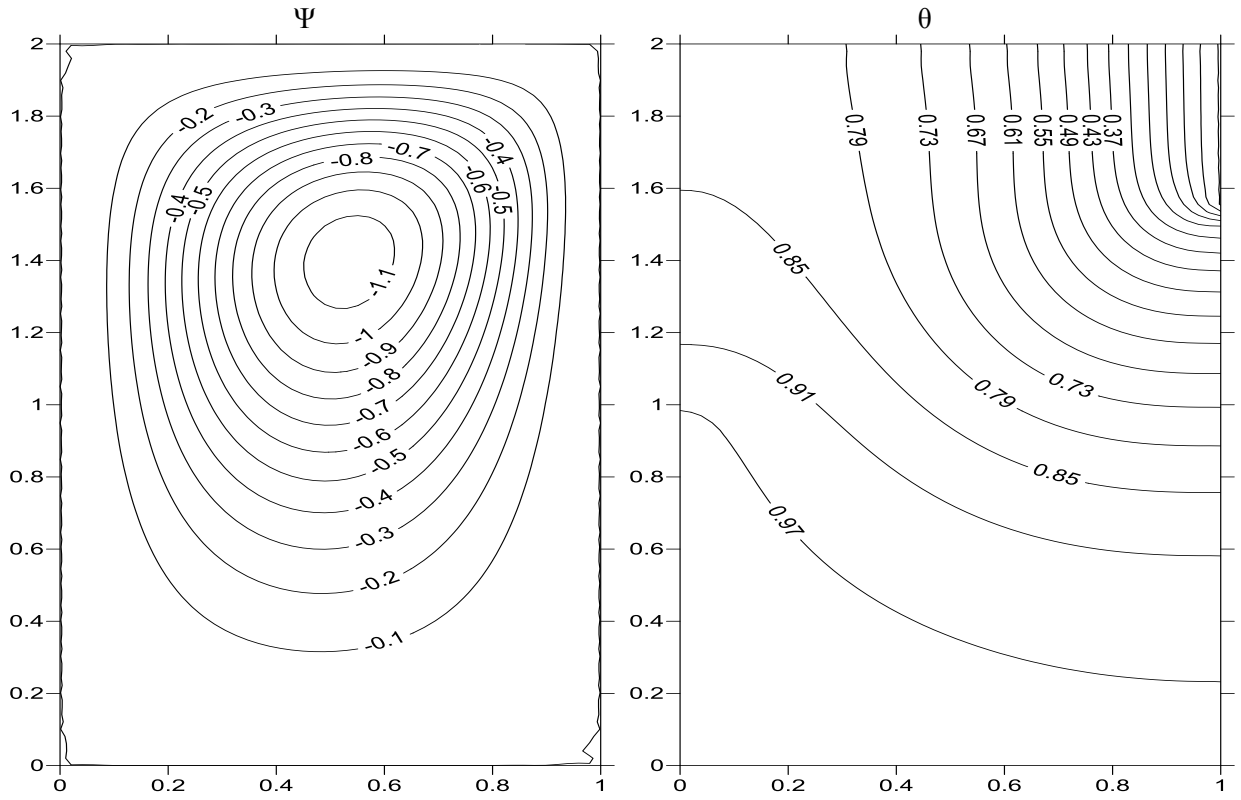

(b) AR = 2

Figure 4. Streamline (Ψ) and isotherm (θ) contours of bottom-top case for various aspect ratios and [Ra $=10^3$, $L_h = 0.5$ and $L_c = 0.25$].

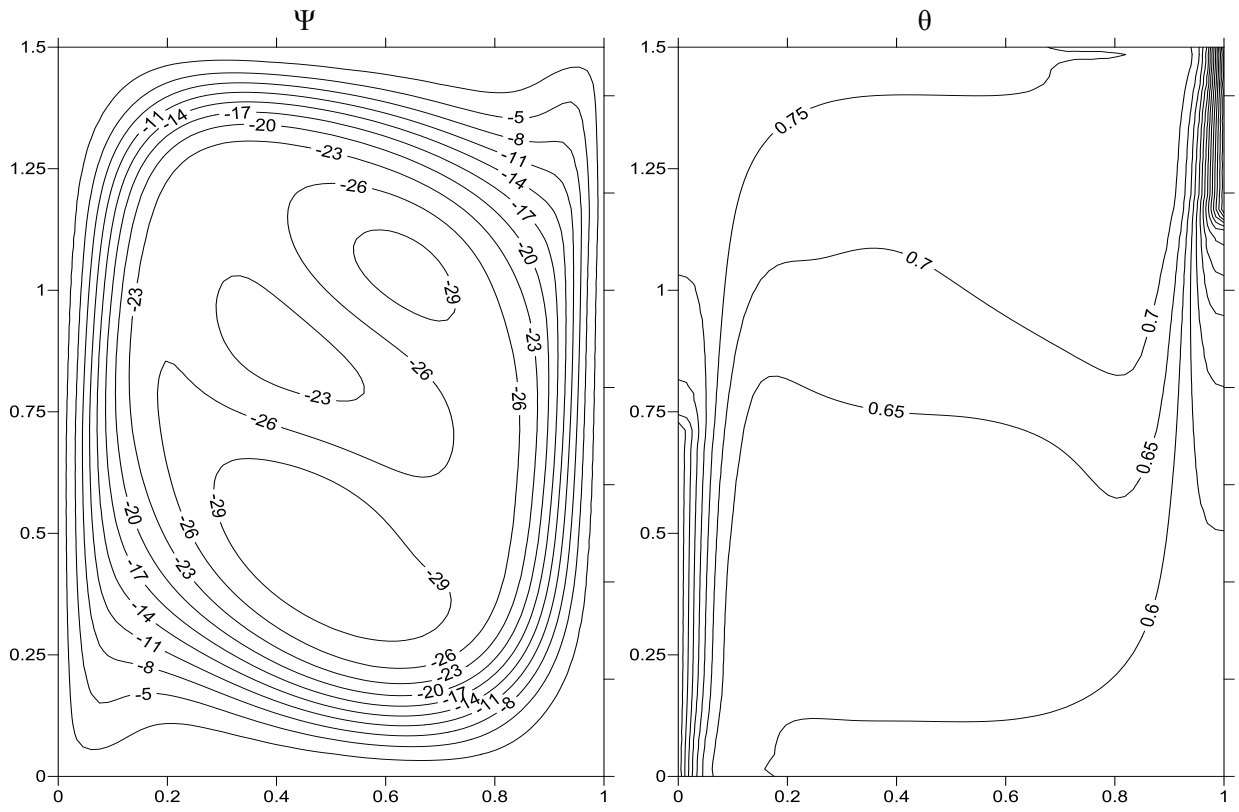

(a) AR = 1.5

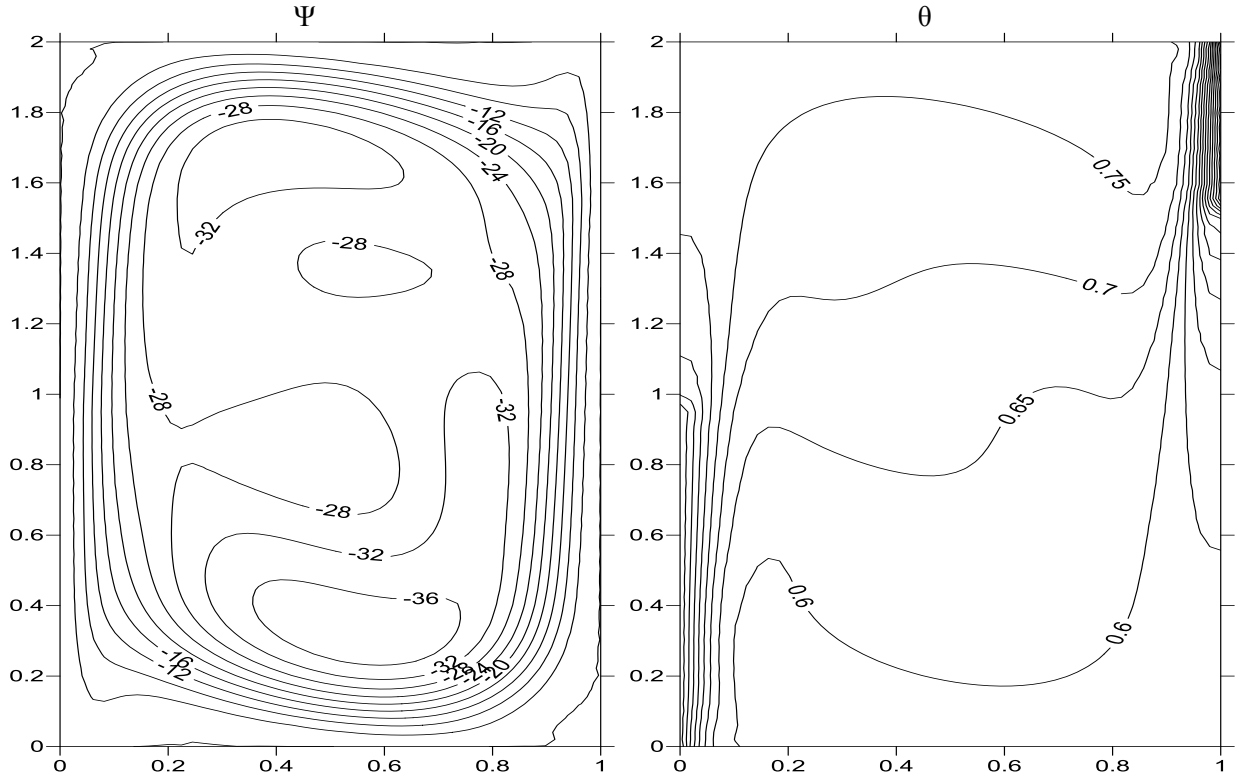

(b) AR = 2

Figure 5. Streamline (Ψ) and isotherm (θ) contours of bottom-top case for various aspect ratios and [Ra =10^6, L_h = 0.5 and L_c = 0.25].

C- Effect of the dimensionless heat sources length

Figures 6 and 7 explain the streamline (Ψ) and isotherm (θ) contours for (B-T) case at various (AR), (Ra) and dimensionless hot and cold source lengths. In Figures 6 and 7 when ($Ra = 10^3$ and $Ra = 10^6$) and aspect ratio [AR = 1], it can be seen that the change in lengths of sources from [$L_h = 0.75$ to $L_h = 0.25$] and [$L_c = 0.25$ to $L_c = 0.75$], lead to represent the flow by a major vortices and the stream function values increased also. It increased from [$|\Psi|_{max} = 0.46$] to [$|\Psi|_{max} = 1.1$] as shown in Figure 6, while increase from [$|\Psi|_{max} = 19$] to [$|\Psi|_{max} = 20$] as shown in Figure 7. In general, it can be concluded from the results presented in Figure 6 that the streamlines represented by flow vortices one uniform and cover the entire zone of the cavity. In this figure the effect of dimensionless length of heat sources is not too effective. Since the dominant mode of heat transfer is the conduction.

From the opposite side, a different style of behavior can be detected in Figure 7. In these figure the flow vortices are affected by variation in (L_h) and (L_c). Since in this case the convection is the main method to transfer the heat inside the cavity.

For isotherms, it can be noticed that the increase in (L_c) from [$L_c = 0.25$] to [$L_c = 0.75$] and the decrease in (L_h) from [$L_h = 0.75$] to [$L_h = 0.25$] lead to extend the isotherms along the cold upper region. While, it decreases them in the hot lower region. This behavior can be noticed in Figures 6 and 7.

4.2 Case two (top-bottom)

A- Effect of Rayleigh number

Figure 8 illustrate streamline (Ψ) and isotherm (θ) contours for different values of (Ra) and for [AR = 1, $L_h = 0.5$ and $L_c = 0.25$]. From these figures, it can be seen that when the Rayleigh number begin with ($Ra = 10^3$). The values of stream function increase increased to maximum value. It increasing from [$|\Psi|_{max} = 0.39$] at [$Ra = 10^3$] to [$|\Psi|_{max} = 19$] at [$Ra = 10^6$]. This increasing in the values of the stream function refer to the effecting of the convection when the Rayleigh number increasing. In fact, the heat transferred from the hot region beside the vertical sidewalls and it moves beside the cold region in the upper part of the right sidewall before it reaches to the adiabatic bottom wall. This motion of rotation the flow leads to forming the convection vortices as shown in Figure 8. The vortices began with high values in the core of cavity and then decreasing due to no slip condition. Also, in this case appeared the miner vortices are seen in the left upper and right lower corners of the cavity.

With respect to isotherm contours (θ), in Figure 8 the uniform in shape and parallel each to other, this can be seen in the low value of the Raleigh number. This indicate that the controlling of the conduction in this value [i.e., $Ra = 10^3$]. It can be seen that the isotherm are high adjacent to the hot wall where the thermal source is installing and then lowered towards the cold thermal source. Nut with increasing the Rayleigh number value, the isotherms began to confuse specially at middle, this due to the significant effect of the convection.

B- Effect of aspect ratio of the cavity

Figures 9 and 10 illustrate streamline (Ψ) and isotherm (θ) contours for various values of aspect ratio. At ($Ra = 10^3$) as shown in Figure 9, the flow field was represented by major uniform vortices. With increasing from [AR = 1.5] to [AR = 2], the stream function values have been increased from [$|\Psi|_{max} = 0.22$] to [$|\Psi|_{max} = 0.6$].This appeared that the flow field was enhanced by increasing the (AR).

For isotherm contours, it can see from the increasing of the aspect ratio does not significant effect on these contours. This is due to the low values of (Ra) [i.e. $Ra = 10^3$], in this case, the heat transfer is controlled by the conduction.

With respect to Figure 10, it can be seen that the stream function value decreasing with increasing of (AR) from [$|\Psi|_{max} = 40$] at [AR = 1.5] to [$|\Psi|_{max} = 24$] at [AR = 2].The flow field which filled the entire cavity which represented by major and minor vortices. Also, the vortices more extended towards the upper region of the cavity filled entire cavity comparing with previous shape in Figure 9. This due to high value of the (Ra) reaches to [$Ra = 10^6$].

C- Effect of the dimensionless heat sources length

Figures 11 and 12 showed the streamline (Ψ) and isotherm (θ) contours for the top-bottom case at various values of (Ra) and (AR=1) and dimensionless hot and cold heat source lengths. When (Ra) is low [$Ra = 10^3$], it can be seen a similar behavior of the flow field between the two figures. Now, when the length of hot source decreases and the cold source increases, [i.e., $L_h = 0.75$] to [$L_h = 0.25$] and [$L_c = 0.25$] to [$L_c = 0.75$] the values of stream function begin to increase. So, it increase from [$|\Psi|_{max} = 0.4$] to [$|\Psi|_{max} = 1.0$] at

[Ra = 10^3] as shown in Figure 11. While, it increase from [$|\Psi|_{max}$ = 25] to [$|\Psi|_{max}$ = 42] at [Ra = 10^6] as shown in Figure 12. Therefore, it can be seen improved the flow in this case with decreasing in the hot source length and the increasing in the cold source length.

With respect to isotherms, in general, it is found symmetrical and parallel to each other .This behavior can be seen for different values of (AR) as shown in Figure 11. Furthermore, it can be seen that when the cold source length longer the hot source a good distribution of isotherms from the hot source to the cold one can be noticed.

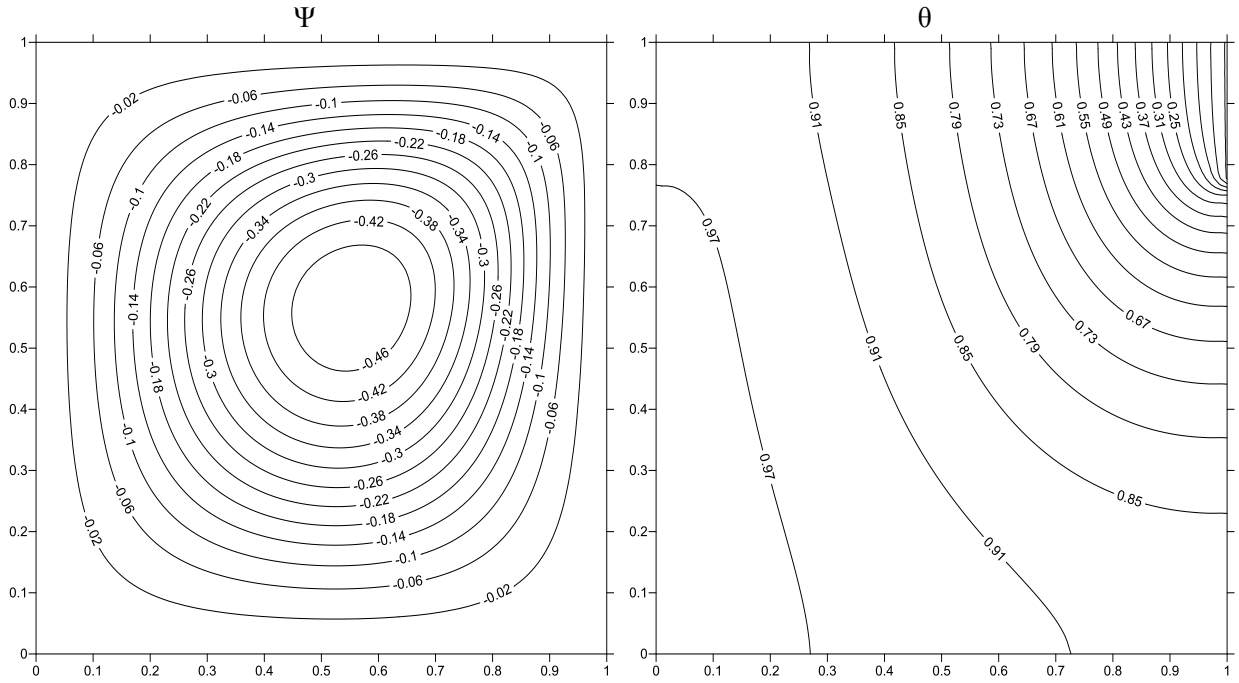

(a) L_h = 0.75 and L_c = 0.25

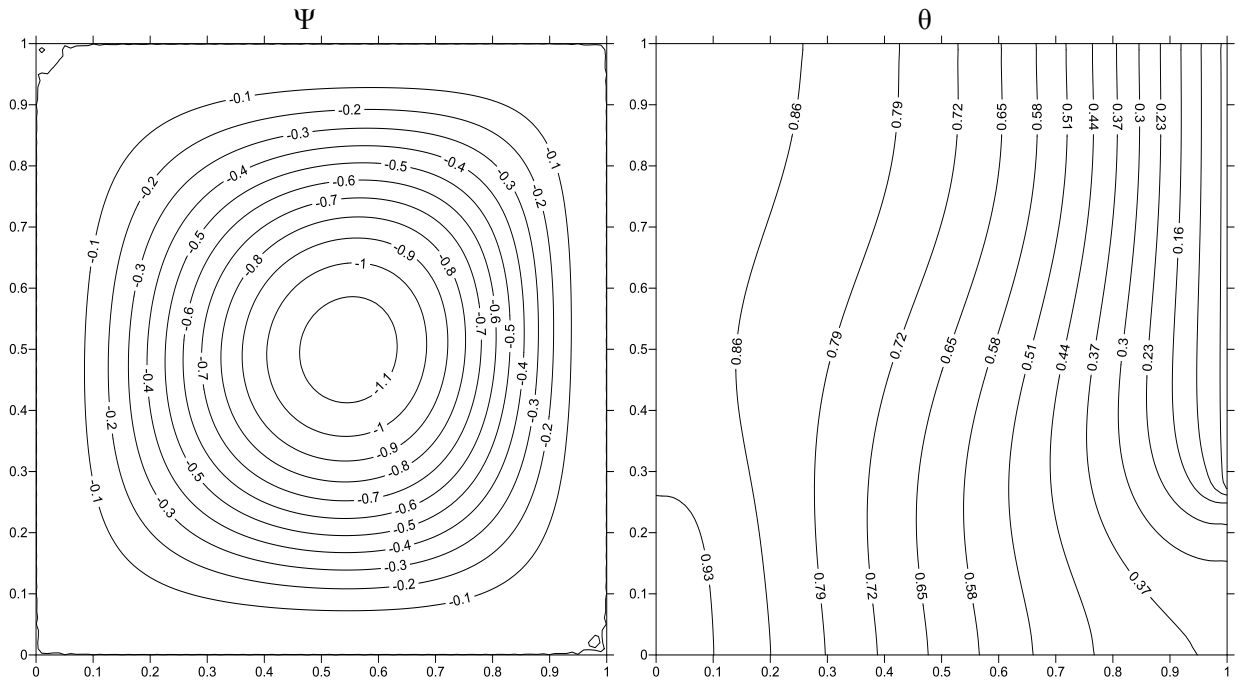

(b) L_h = 0.25 and L_c = 0.75

Figure 6. Streamline (Ψ) and isotherm (θ) contours of bottom-top case for various hot and cold heat source lengths and [Ra =10^3 and AR = 1].

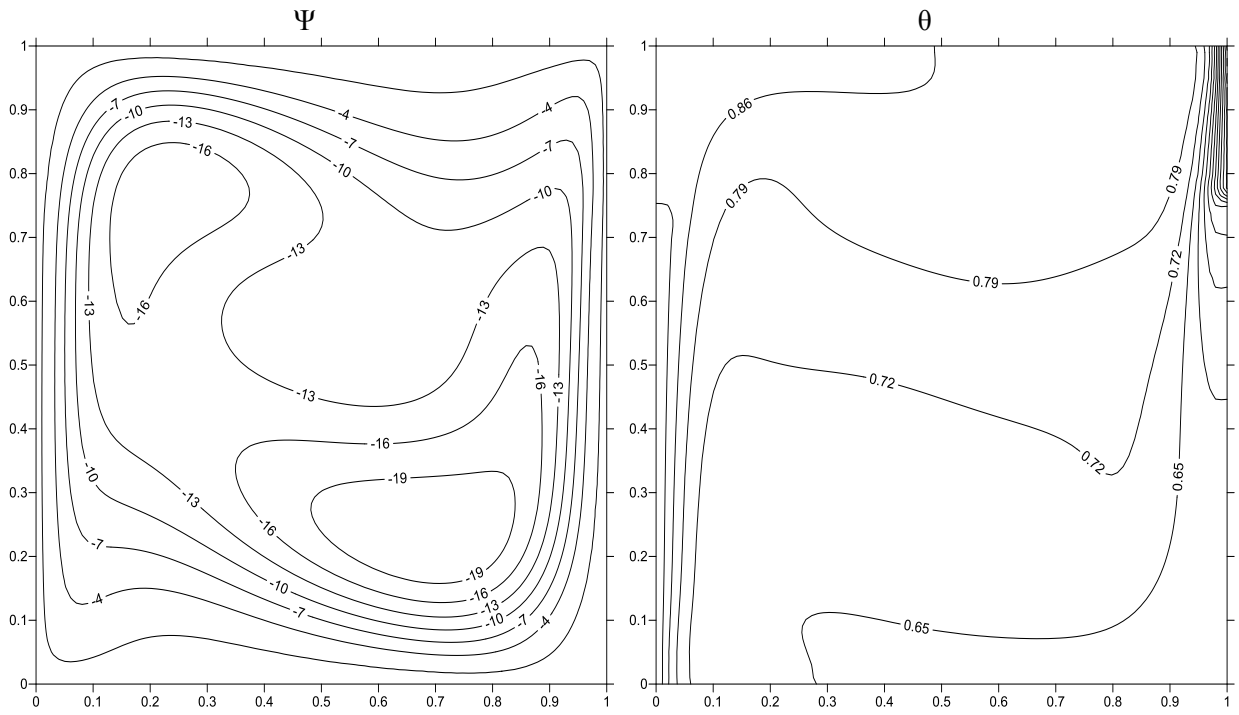

(a) $L_h = 0.75$ and $L_c = 0.25$

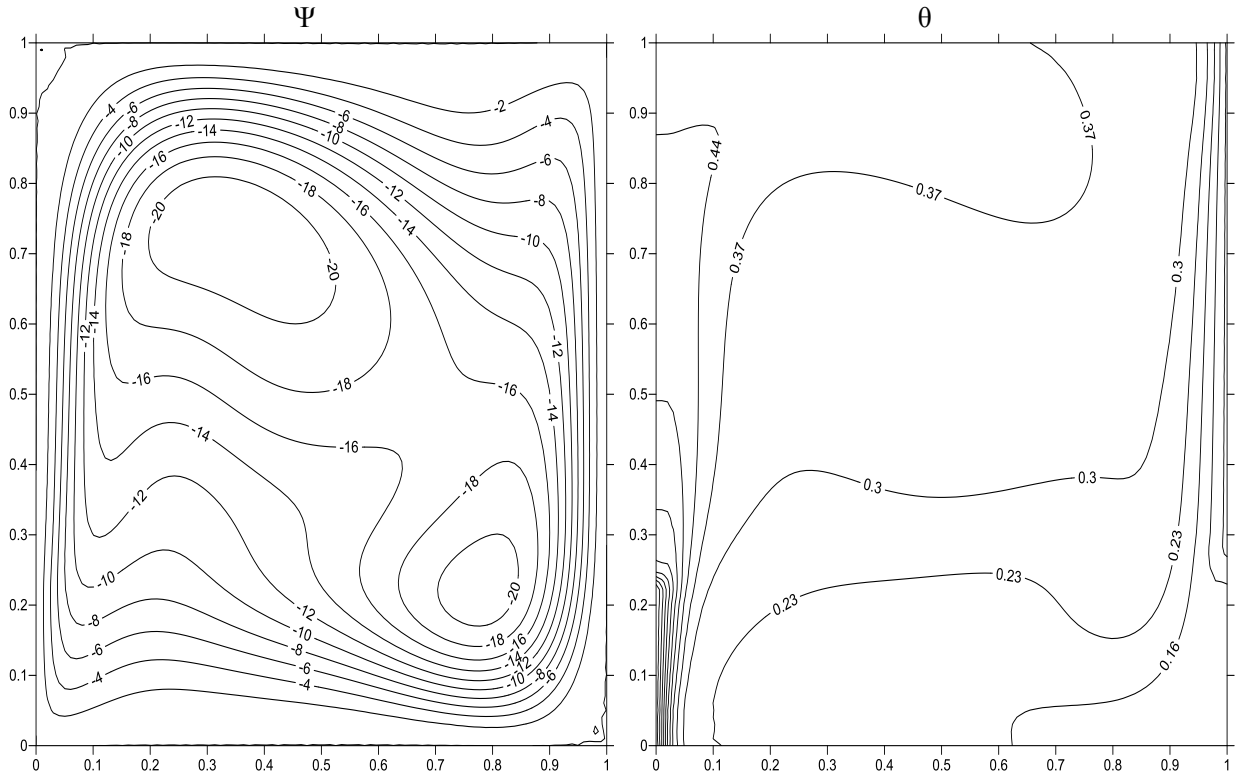

(b) $L_h = 0.25$ and $L_c = 0.75$

Figure 7. Streamline (Ψ) and isotherm (θ) contours of bottom-top case for various hot and cold heat source lengths and [Ra =10^6 and AR = 1].

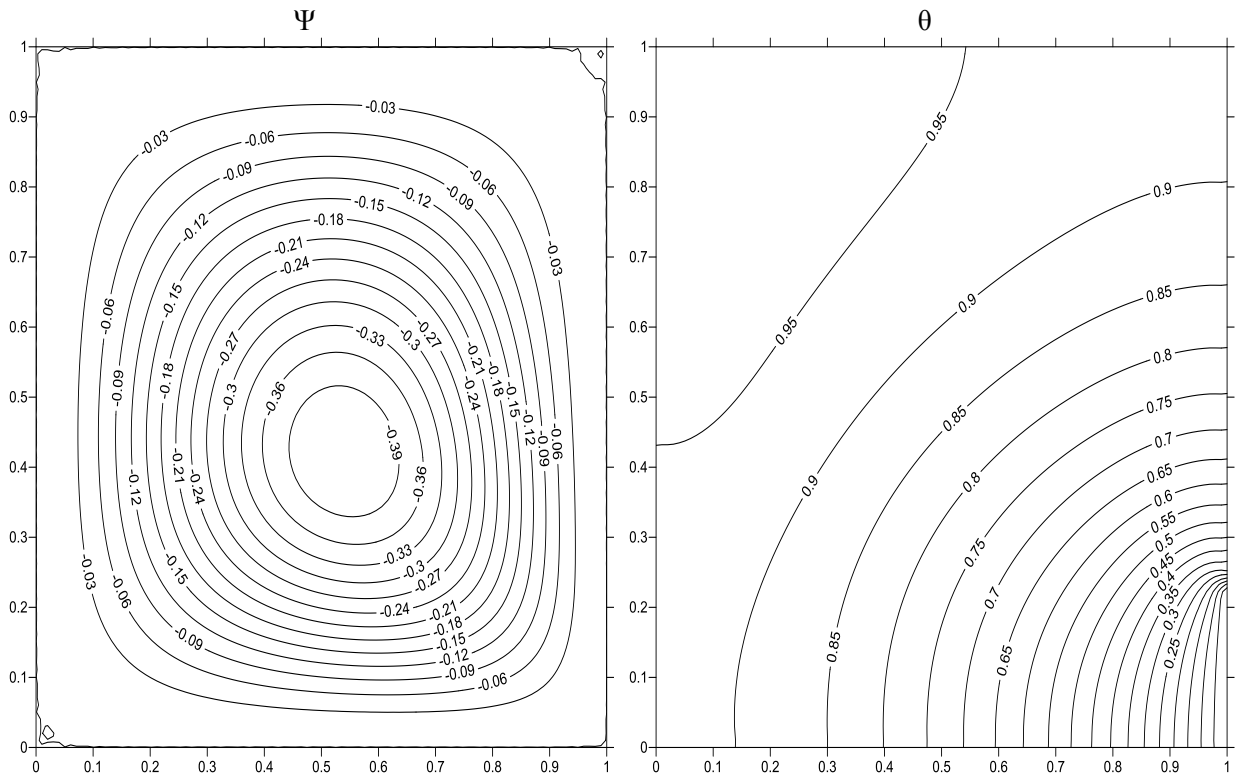

(a) Ra = 10^3

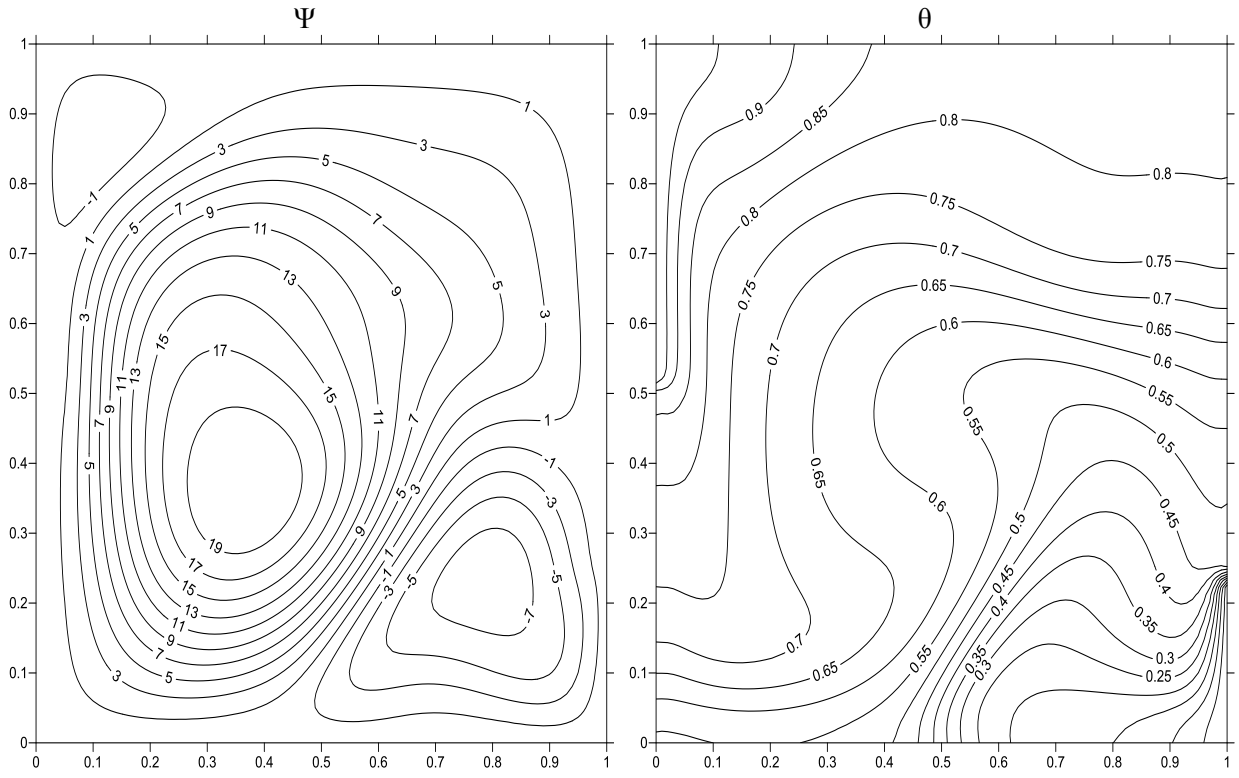

(b) Ra = 10^6

Figure 8. Streamline (Ψ) and isotherm (θ) contours of top-bottom case for various Rayleigh number and [AR=1, L_h = 0.5 and L_c = 0.25].

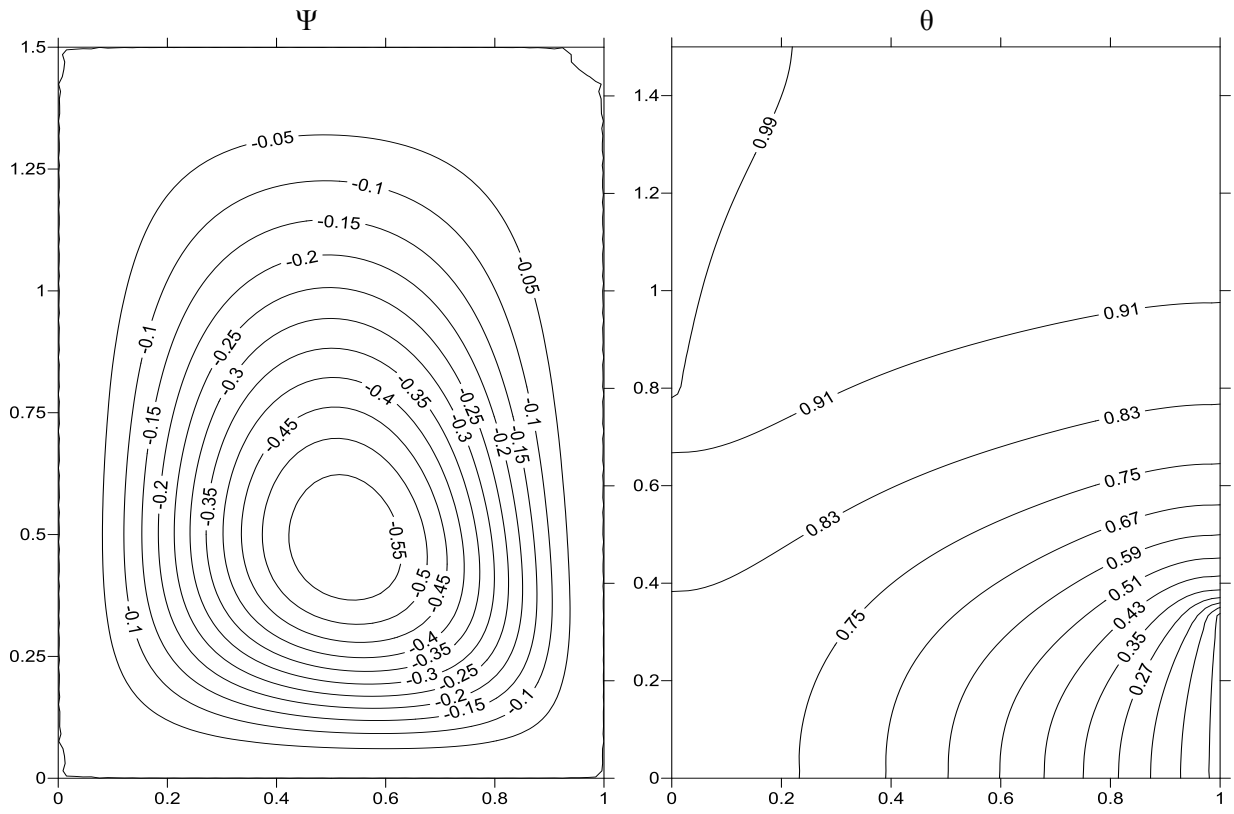

(a) AR= 1.5

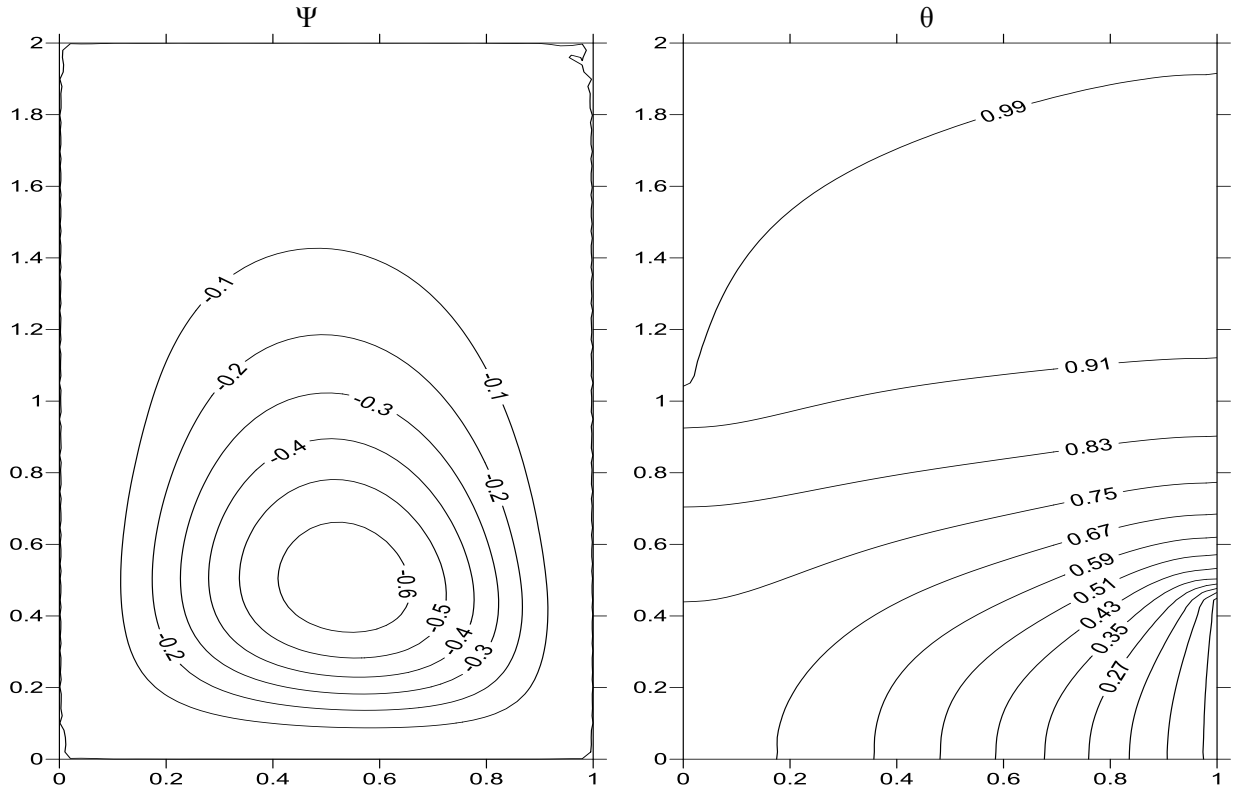

(b) AR= 2

Figure 9. Streamline (Ψ) and isotherm (θ) contours of top -bottom case for various aspect ratios and [Ra =10^3, L_h = 0.5 and L_c = 0.25].

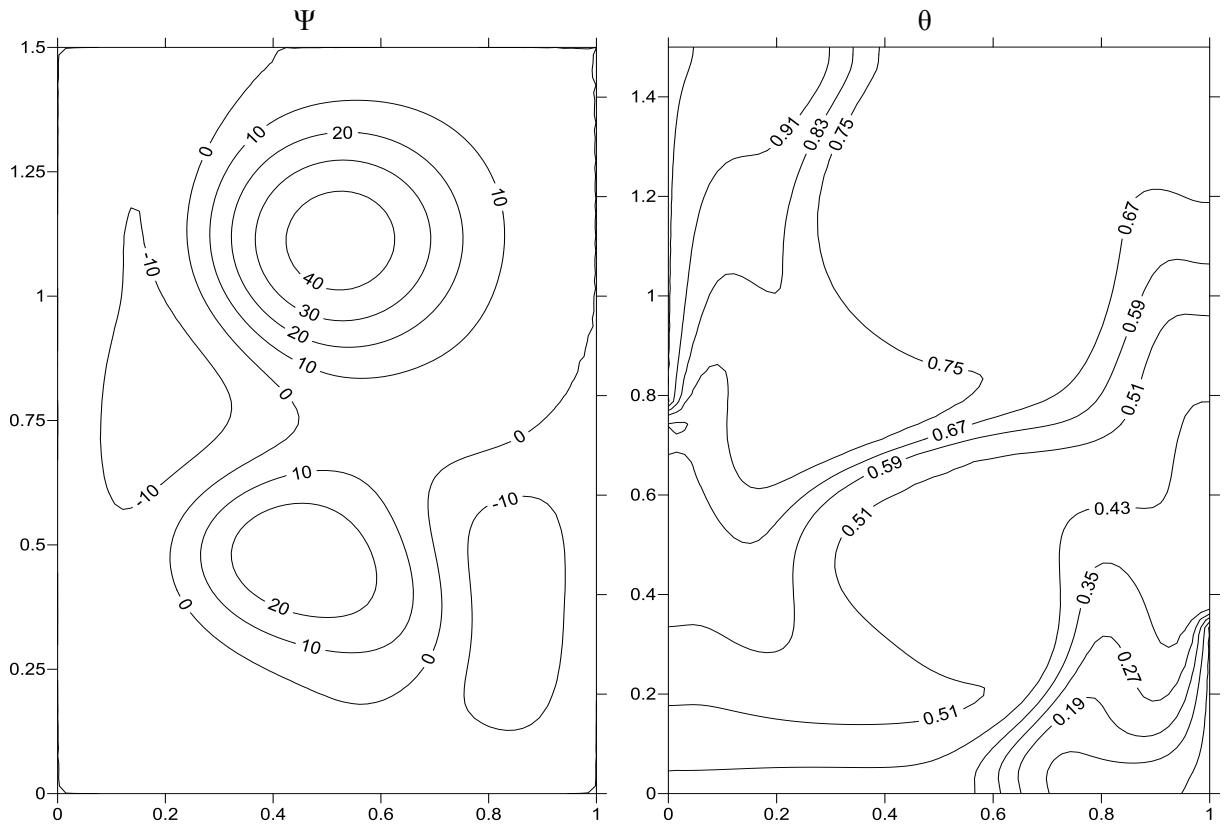

(a) AR= 1.5

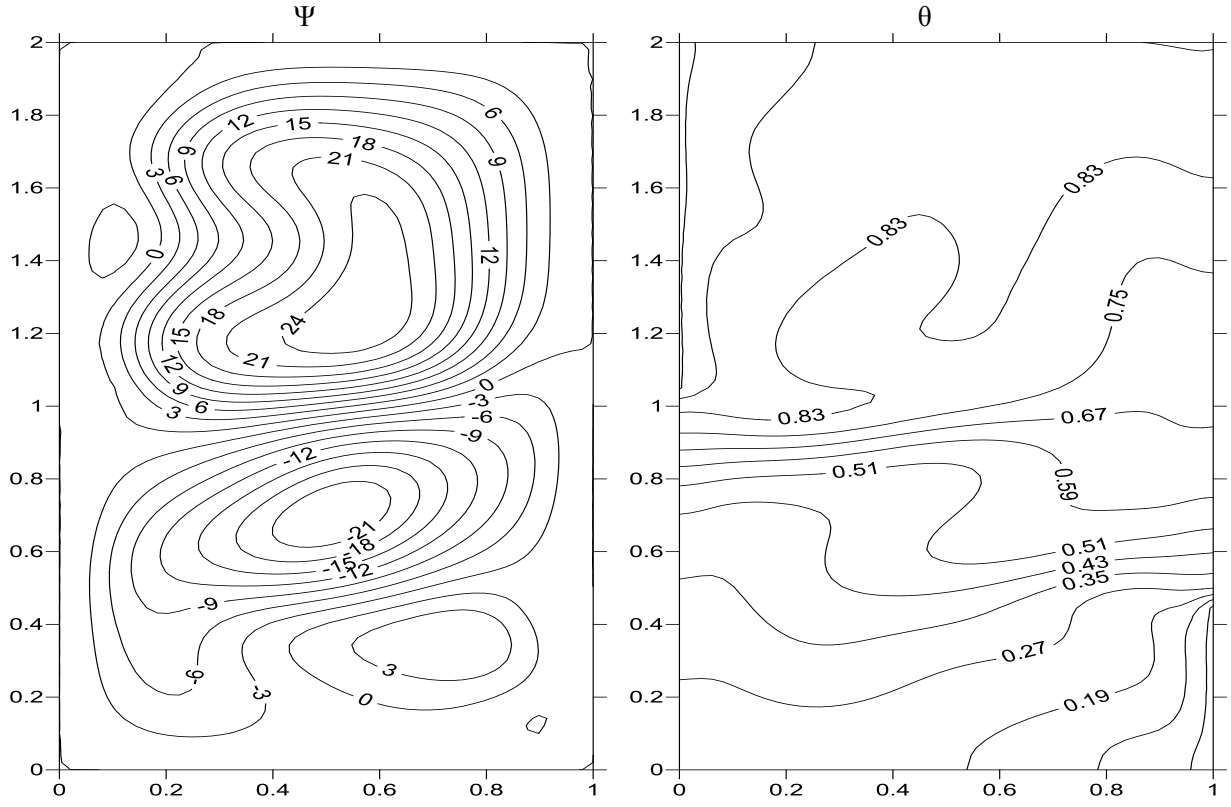

(b) AR= 2

Figure 10. Streamline (Ψ) and isotherm (θ) contours of top -bottom case for various aspect ratios and [Ra =10^6, L_h = 0.5 and L_c = 0.25].

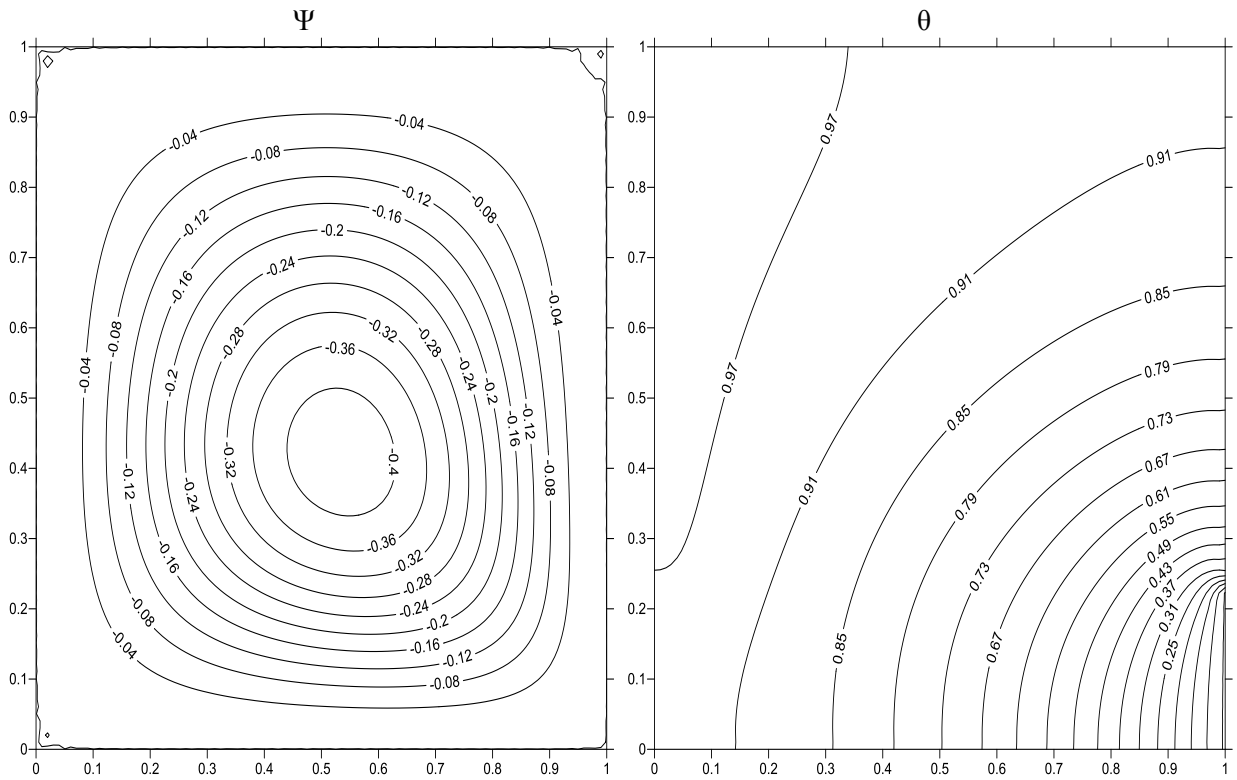

(a) $L_h = 0.75$ and $L_c = 0.25$

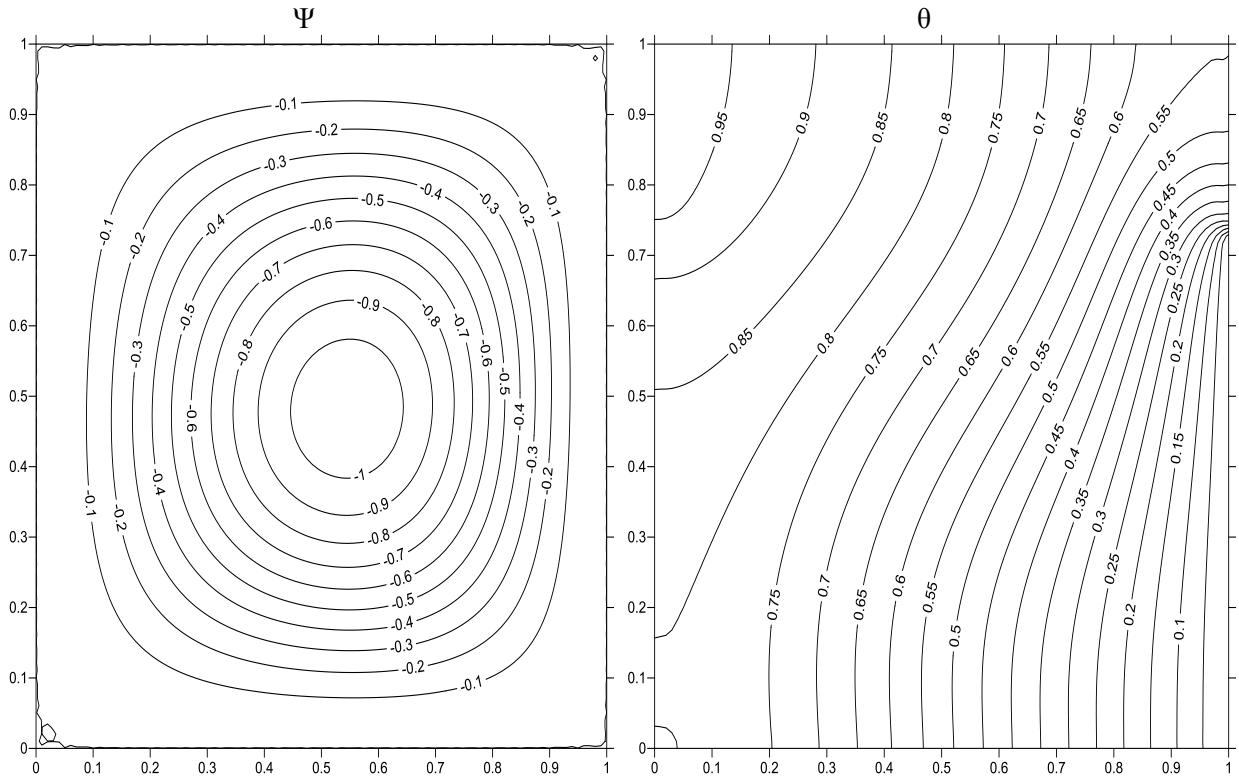

(b) $L_h = 0.25$ and $L_c = 0.75$

Figure 11. Streamline (Ψ) and isotherm (θ) contours of top-bottom case for various hot and cold heat source lengths and [Ra =10^3 and AR = 1].

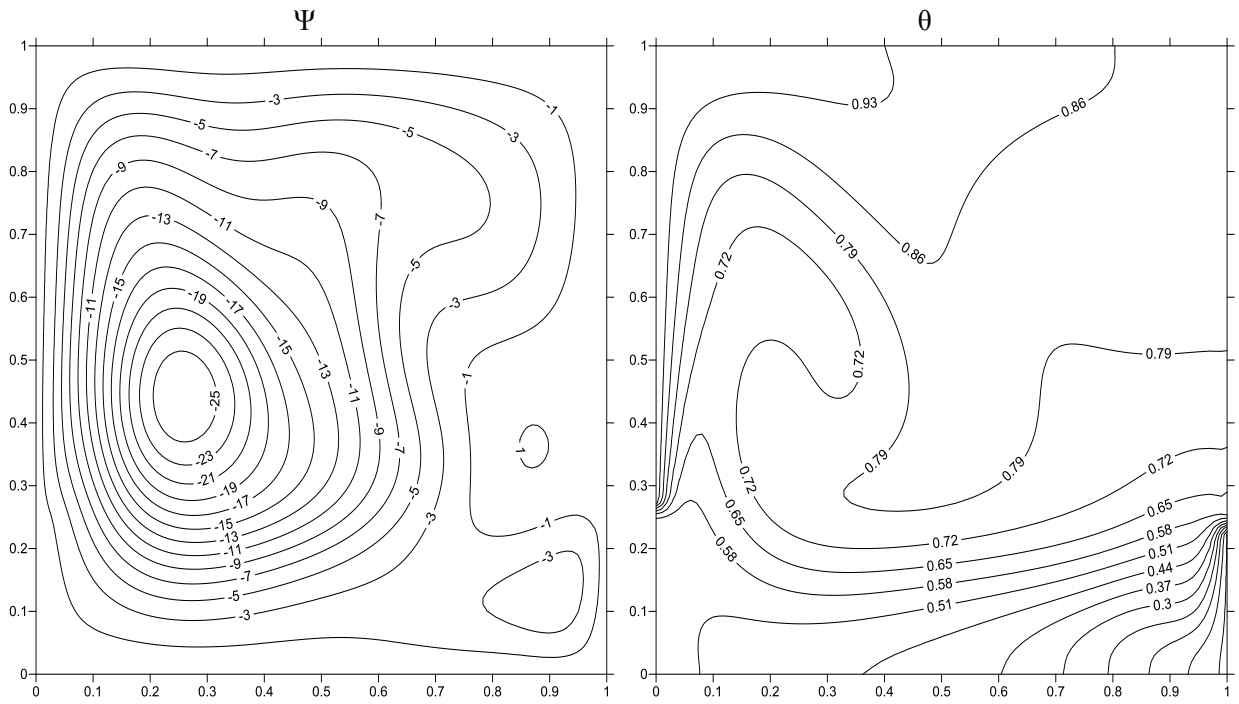

(a) $L_h = 0.75$ and $L_c = 0.25$

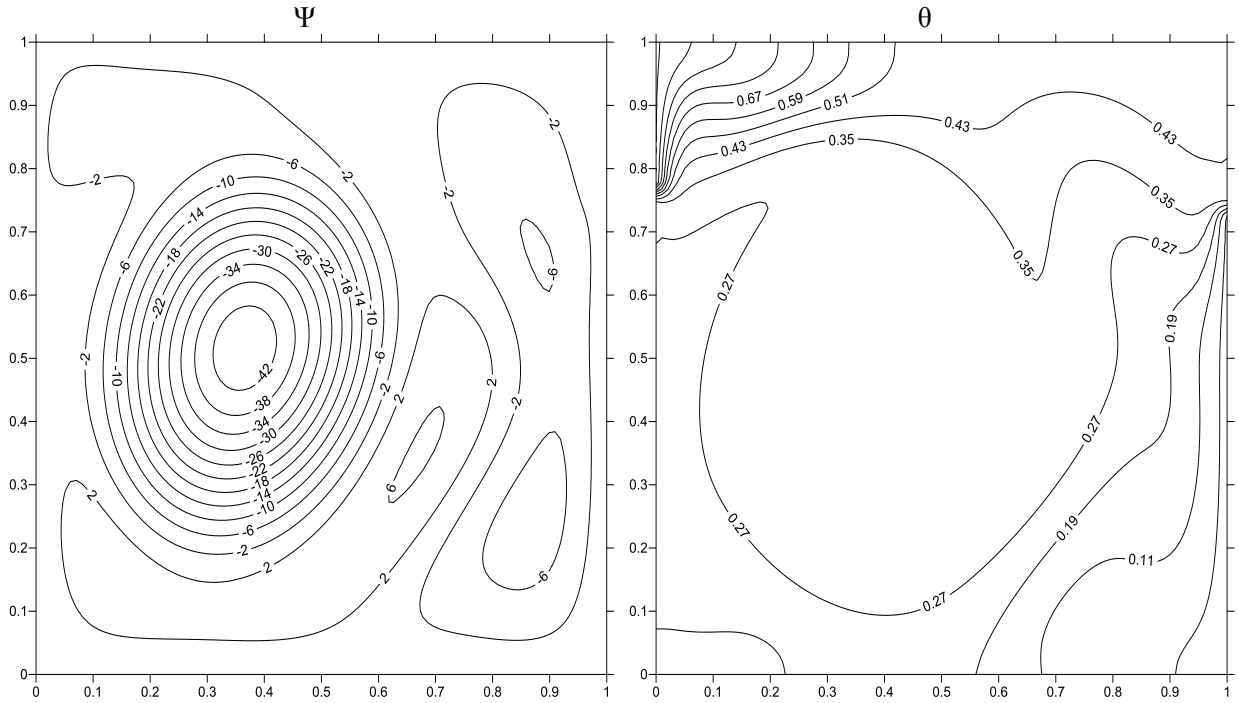

(b) $L_h = 0.25$ and $L_c = 0.75$

Figure 12. Streamline (Ψ) and isotherm (θ) contours of top-bottom case for various hot and cold heat source lengths and [Ra =10^6 and AR = 1].

4.3 local Nusselt number results

Figure 13 present the local Nusselt number profile (Nu) along the hot wall of the (B-T) case for different values of Rayleigh number and [AR = 1, $L_h = 0.5$, $L_c = 0.25$]. As expected, the values of (Nu) increase as (Ra) increases. This due to the increase in the effect of the force of the natural convection when (Ra) increase from [Ra = 10^3] to [Ra = 10^6] respectively. Therefore, it can be concluded that the rate of the heat transfer is increased when the (Ra) increases.

The profile of the local Nusselt number along the hot wall (Nu) are shown in Figure 14 for different values of the aspect ratio and [Ra = 10^3 to Ra = 10^6, L_h = 0.5, L_c = 0.25]. Therefore, it can be concluded that rate of heat transfer is increased when the aspect ratio increased.

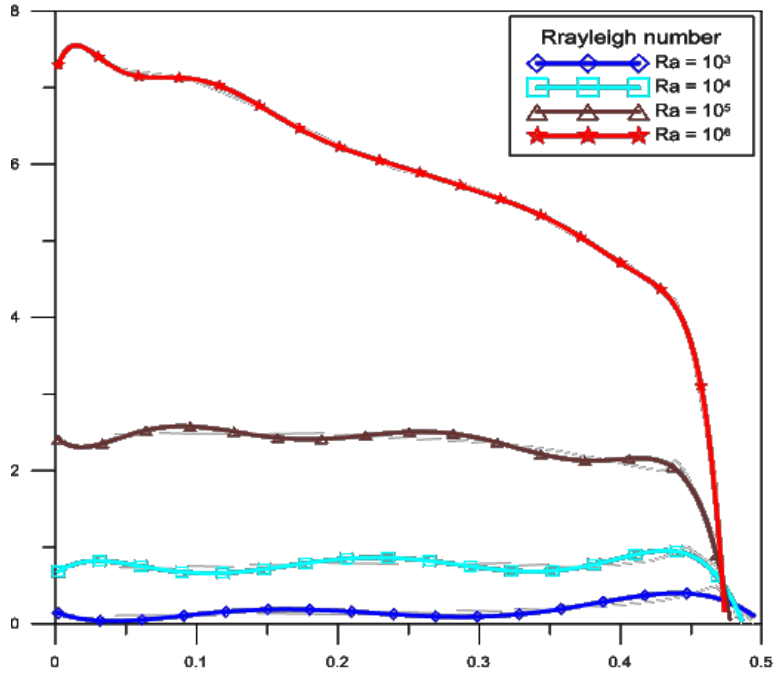

Figure 13. Profile of local (Nu) of bottom – top case for different values of Rayleigh number and [AR = 1, L_h = 0.5 and L_c = 0.25].

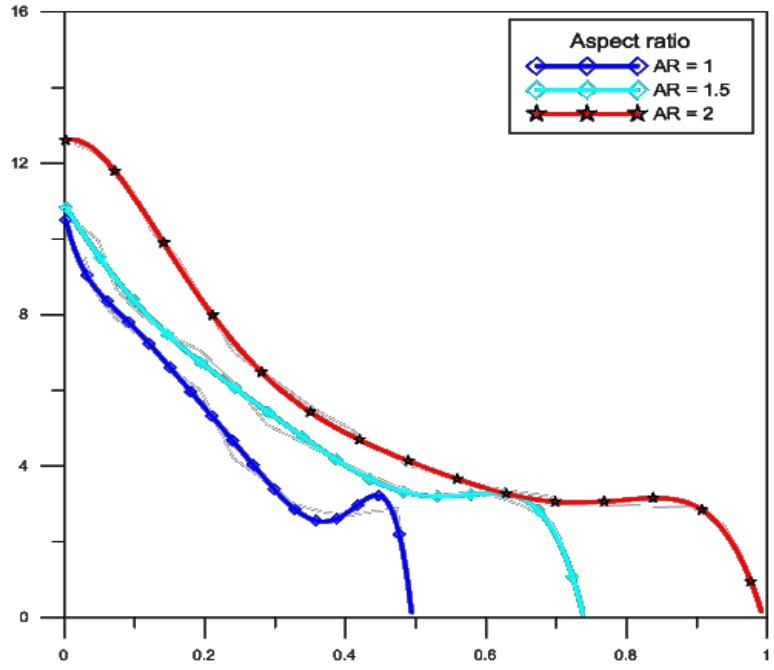

Figure 14. Profile of local (Nu) of bottom – top case for different values of the aspect ratio (AR) and [Ra = 10^6, L_h = 0.5 and L_c = 0.25].

Figure 15 illustrate the (Nu) for different thermal dimensionless source lengths for case (B-T) and [Ra = 10^3 to Ra = 10^6, L_h = 0.5, 0.75 and 0.25, L_c = 0.25 to L_c = 0.75], it can be noticed that in the (B-T) case the values of the (Nu) increase as the dimensionless source length decrease to (L_h = 0.25) of the total length of the vertical sidewall. This due to the convection mode play vital role to transmitted the heat from the hot to cold wall.

Figure 16 present the local Nusselt number profile (Nu) along the hot wall of (T-B) case for different values of Rayleigh number and [AR = 1, L_h = 0.5, L_c = 0.25].As shown in figure below the values of (Nu) increase as (Ra) increases. So the effect of the Rayleigh number effected on the natural convection when (Ra) increase from [Ra = 10^3] to [Ra = 10^6] respectively. Therefore, it can be concluded that the rate of the heat transfer is similar to case one above it increased with increasing of the Rayleigh number.

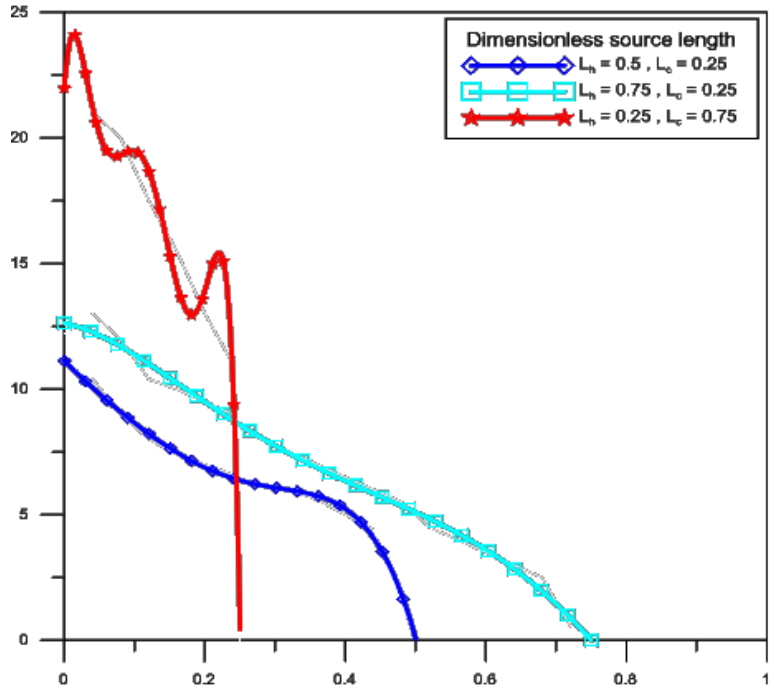

Figure 15. Profile of local (Nu) of bottom –top case for different dimensionless source lengths and [Ra = 10^6, AR =1].

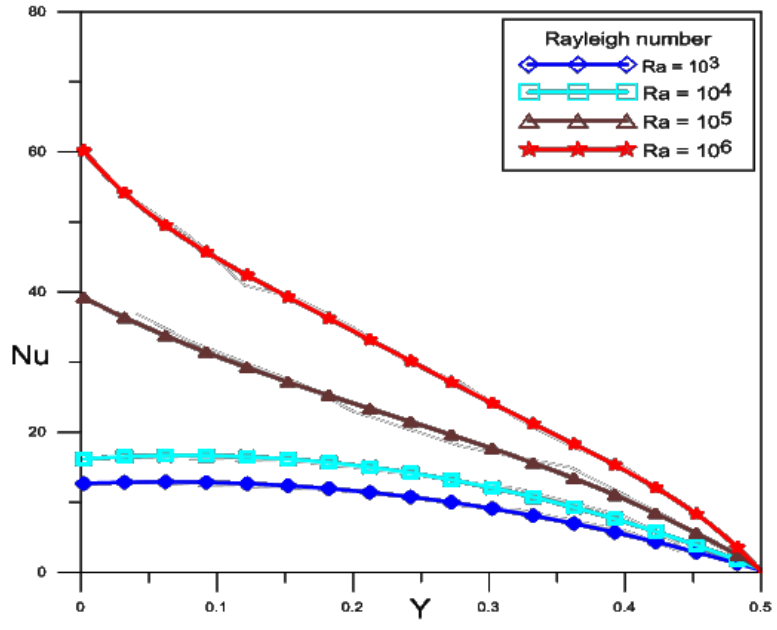

Figure 16. Profile of local (Nu) of top – bottom case for different values of Rayleigh number (Ra) and [AR = 1, L_h = 0.5 and L_c = 0.25].

Figure 17 for (T-B) case with different values of the aspect ratio and [Ra = 10^3 to Ra = 10^6, L_h = 0.5, L_c = 0.25]. From this figure, it can be seen that (Nu) increase with increasing in aspect ratio and in this

case it have been maximum value corresponds to previous (B-T) case. So, it can be concluded that with increasing of the aspect ratio the rate of heat transfer will be increased.
Figure 18 illustrate the (Nu) for different thermal dimensionless source lengths for case (T-B) and [Ra = 10^3 to Ra = 10^6, L_h = 0.5 ,0.75 and 0.25, L_c = 0.25 to L_c = 0.75], it can be noticed that in this case with decreasing the length of the hot source to minimum this lead to increase the Nusselt number [i.e. L_h = 0.25]. This due to effecting role of the convection mode to play a transmitted the heat from the hot wall to cold other.

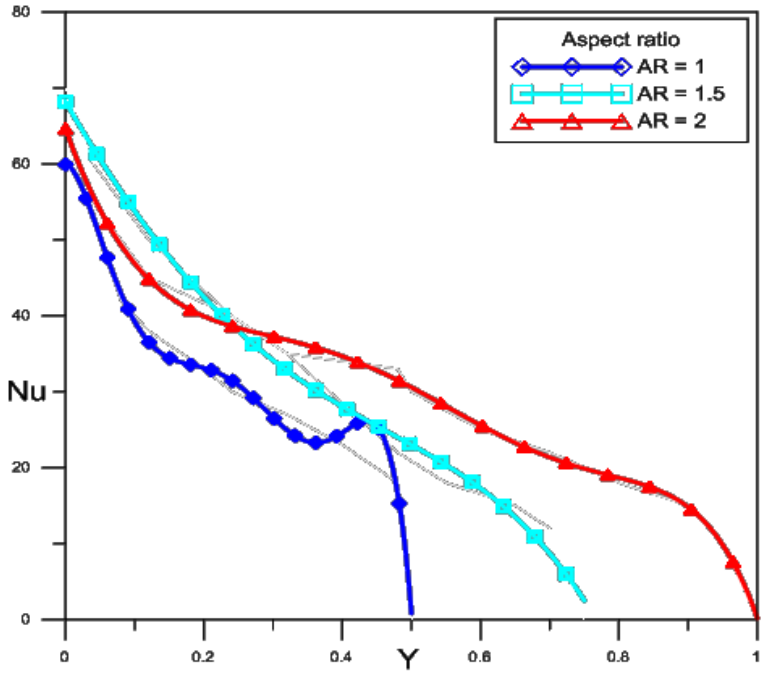

Figure 17. Profile of local (Nu) of top – bottom case for different values of the aspect ratio (AR) and [Ra = 10^6, L_h = 0.5 and L_c = 0.25].

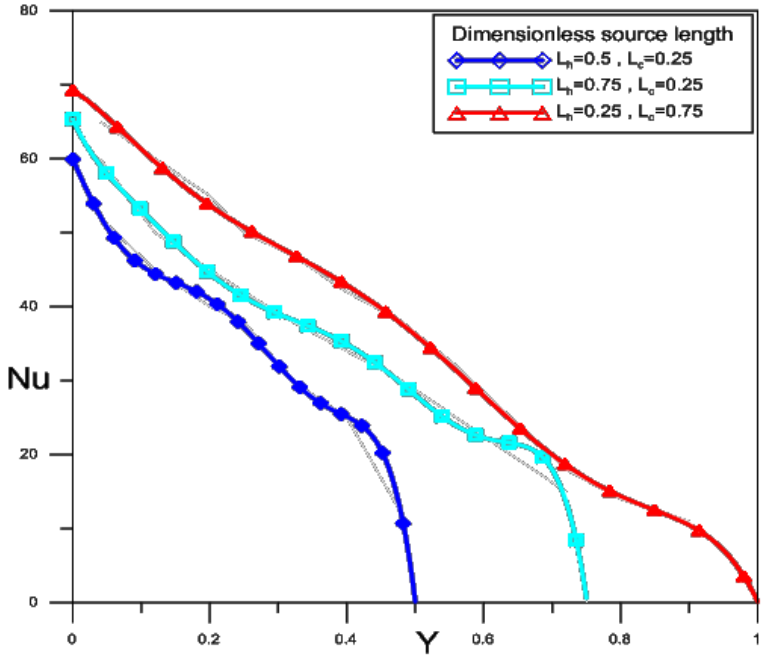

Figure 18. Profile of local (Nu) of top –bottom case for different dimensionless source lengths and [Ra = 10^6, AR =1].

5. Conclusions

The following points summarize the most important conclusions related with the current study.

1- It has been noticed that, with the increase of Rayleigh number, aspect ratio and dimensionless thermal source lengths, the intensity of the fluid flow and the convection heat transfer increase.
2- For these cases, the natural convection is dominant at [Ra = 10^3 to Ra = 10^6].
3- In both cases (B-T) and (T-B), the isotherm lines become curved and curvy with increasing the Rayleigh number and the aspect ratio.
4- From the results of the present work, it can be concluded that the case two (T-B) gives the higher heat transfer enhancement than the first one.
5- The Nusselt number increases with the increasing of the Rayleigh number, the aspect ratio and when the length of the thermal hot source is the less than the cold source.

Nomenclature

Symbol	***Description***	***Units***
AR	Aspect ratio of the cavity (H/W)	-----
c_p	Constant pressure specific heat	J /kg.K
D	Location of the dimensionless heater	-----
E	size of the dimensionless heater	-----
Gr	Grashoff Number	-----
g	Gravitational acceleration	m /s^2
H	Height of cavity	m
h	Convection heat transfer coefficient	W/m^2.K
k	Effective thermal conductivity	W/m.C°
L_s	Dimensionless length of the heat source	-----
Nu	Local Nusselt number ($\frac{h * L_s}{k}$)	-----
Nu_{av}	Average Nusselt number	-----
P	Pressure	Pa
P_r	Prandtl number	-----
q"	Heat flux per unit area	W / m^2
Ra	Rayleigh number ($Ra = \frac{g\beta(T_h - T_c)H^3 P_r}{\nu^2}$)	-----
T	Temperature	K
U	Dimensionless velocity component in X-direction	-----
u	Dimensional velocity component in x-direction	m /s
V	Dimensionless velocity component in Y-direction	-----
v	Dimensional velocity component in y-direction	m /s
W	Width of cavity	m
X	Non- dimensional coordinate in horizontal direction (x/W)	-----
x	Cartesian coordinate in horizontal direction	m
Y	Non-dimensional coordinate in vertical direction (y/H)	-----
y	Cartesian coordinate in vertical direction	M

Greek Symbol	***Description***	***Units***
α	Thermal diffusivity of the fluid ($k/\rho.c_p$)	m^2/s
ν	Kinematic viscosity of fluid	m^2/s
β	Coefficient of thermal expansion	1/K
Ω	vortisty	
θ	Dimensionless temperature distribution [$(T-T_c)/\Delta T$]	-------
ψ	Stream function	m/s^2
Ψ	Dimensionless stream function	-----
Subscripts and superscripts		
c	Cold	-----
h	Hot	-----
av	Average	-----
i, j	Unit vector in x and y directions	-----

Abbreviations		
FDM	Finite Difference Method	-----
SUR	Successive Under Relaxation	-----
B-T	Bottom - Top	-----
T-B	Top-Bottom	-----

References

[1] Kane, M., Mmbow,C., Sow,M. and Sarr, J., "A Study on Natural Convection of Air in a Square Cavity With Partially Thermally Active Side Walls " Journal of Fluid Dynamic, Vol. 7, 2017,pp. 623-641.

[2] Jawad, Q., "Numerical investigation on The Effect of Inclination Angle on Natural Convection Heat Transfer in A Rectangular enclosure" Journal of Engineering and Development, Vol. 17, 2013, pp.128-140.

[3] Cianfrini, C., Corcione, M. and Dellomo, P., "Natural Convection in Tited Square Cavities with Differentially Heated Opposite Walls", International Journal of Thermal Science, Vol. 44, 2005, pp. 441-451.

[4] Basak, T., Roy, S. and Balakrishnan, A., "Effect of Thermal Boundary Conditions on Natural Convection Flows Within a Square Cavity", International Journal of Heat and Mass Transfer. Vol. 49, 2006, pp. 4525-4535.

[5] Hussein, A. and Hussain, S., "Numerical analysis of steady natural convection of water in inclined Square Enclosure with Internal Heat generation", International Conference on Mechanical and Electrical Technology, 2010, pp. 502-508.

[6] Turan, O., Poole, R. and Chakraborty, N., "Influences of Boundary Conditions on Laminar Natural Convection in Rectangular Enclosures with Differentially Heated Side Walls", International Journal of Heat and Fluid Flow.,Vol.33, 2012, pp.131-146.

[7] Bhattachrya, P. and Das, S., "A Numerical Study of Laminar Natural Convection Heat Transfer Inside a Closed Cavity With Different Aspect Ratio", U.P.B.Sci.Bull., Vol. 77, 2015, pp. 1454-2358.

[8] Hasnaoui, M., Bilgen, E. and Vasseur, P., "Natural Convection Heat Transfer In Rectangular Cavities Partially Heated From Below", Journal of The Thermophysics and Heat Transfer, Vol.6, No.2, 1992, pp.255-264.

[9] Calcagni, B., Marsil, F. and Paroncini, "Natural Convection Heat Transfer in Square Enclosures Heated From Below", Applied Thermal Engineering, Vol.25, 2005, pp. 2522-2531.

[10] Nasr, K., Chouikh, R., Kerkeni, C. and Guizani, A. "Numerical study of The Natural Convection in Cavity Heated from the Lower Corner and Cooled from the Ceiling", Applied Thermal Engineering, Vol.26, 2006, pp. 772-775.

[11] Cheikh, N., Ben beya, B. and Lili, T., "Influence of Thermal Boundary Conditions on Natural Convection In a Square Enclosure Partially Heated From Below", International Journal of Heat and Mass Transfer,Vol.34, 2007, pp. 369-379.

[12] Tabet, S., Dellil, A. and Azzi, A., "Natural Convection in Partially Heated Square Cavity", MECHANIKA, Vol. 22(2), 2016, pp. 119-124.

[13] Turkoglu, H. and Yucel, N, "Effect of Heater and Cooler Locations on National Convention in Square Cavities ", Numerical Heat Transfer, Vol. 27, 1995, pp. 351-358.

[14] Kandaswam, P., Nithyadevi, N. and Ng, C., "Natural Convection in Enclosures with Partially Thermally Active Side Walls Containing Internal Heat Sources", Physics of Fluids, Vol. 20, 2008, pp.1-9.

[15] Alam,P. ,Kumar , A., Kapoor , S. and Ansari, S., "Numerical Investigation of Natural Convection in a Rectangular Enclosure Due to Partial Heating and Cooling at Vertical Walls", communication nonlinear science and numerical simulation, Vol. 17, 2012, pp. 2403-2414.

[16] Djoubeir, D., Omar, K., Soufien, C. and Saddooun, B., "Numerical Simulation of Natural Convection in a Square Cavity with Partially Active Vertical and Horizontal Walls", Integer Programming and Combinatorial Optimization IPCO-2014, Vol. 2, pp.1-6.

[17] Mahapatra, P., Manna,N. and Ghosh , K .,"Effect of Active Wall Location In a Partially Heated Enclosure", International Communications In Heat Transfer , Vol. 61, 2015, pp. 69-77.

[18] Turkoglu, H. and Yucel, N., "Natural Convection in Rectangular Enclosures With Partial Heating and Cooling ", Wairme - und Stoffubertragung ,Vol.29 , 1994 , pp. 471-478.

